

# Direct evidence of terahertz emission arising from anomalous Hall effect

V. Mottamchetty,<sup>1</sup> P. Rani,<sup>2</sup> R. Brucas,<sup>1</sup> A. Rydberg,<sup>1,2</sup> P. Svedlindh,<sup>1,\*</sup> and R. Gupta<sup>1,2,†</sup>

<sup>1</sup>*Department of Materials Science and Engineering,  
Uppsala University, Box 35, SE-751 03 Uppsala, Sweden*

<sup>2</sup>*Department of Physics and Astronomy, Uppsala University, Box 516, SE-75120 Uppsala, Sweden*  
(Dated: February 16, 2023)

A detailed understanding of the different mechanisms being responsible for terahertz (THz) emission in ferromagnetic (FM) materials will aid in designing efficient THz emitters. In this report, we present direct evidence of THz emission from single layer  $\text{Co}_{0.4}\text{Fe}_{0.4}\text{B}_{0.2}$  (CoFeB) FM thin films. The dominant mechanism being responsible for the THz emission is the anomalous Hall effect (AHE), which is an effect of a net backflow current in the FM layer created by the spin polarized current reflected at the interfaces of the FM layer. The THz emission from the AHE-based CoFeB emitter is optimized by varying its thickness, orientation, and pump fluence of the laser beam. Results from electrical transport measurements show that skew scattering of charge carriers is responsible for the THz emission in the CoFeB AHE-based THz emitter.

## I. INTRODUCTION

The region of the electromagnetic spectrum that lies between near microwave and far-infrared radiation is the so-called Terahertz (THz) radiation or THz gap, *i.e.* typically frequencies between 100 GHz and 30 THz. Terahertz radiation finds applications in various fields, such as medicine, security, etc. [1, 2]. Photoconductive switching, optical rectification, transient photo-current in air plasma, and difference frequency generation constitute techniques that are employed for the generation of THz radiation [3–13]. Moreover, THz emission from magnetic materials, utilizing the spin degree of freedom, has recently gained popularity as a promising framework for the generation of broadband radiation without any phonon absorption gaps and with intensity comparable to the standard zinc telluride THz source [14, 15].

There are several possible mechanisms that can explain THz generation in spin-based systems. Beaurepaire *et al.* [16] discovered ultrafast demagnetization (UDM) in 1996, showing that a ferromagnetic (FM) Ni film when demagnetized on a subpicosecond time scale by a femtosecond (fs) laser pulse excitation generates THz radiation [17]. The THz radiation is in this case proportional to the second time-derivative of the magnetization [18] and shows a linear dependence on the thickness of the FM layer. Recently, Kampfrath *et al.* [14, 19] discovered an alternative mechanism for THz generation, which utilizes the inverse spin Hall effect (iSHE) or inverse Rashba Edelstein effect (iREE). Here, the generation mechanism requires a magnetic heterostructure consisting of an FM layer and a non-magnet (NM) layer that possesses a high spin-to-charge (S2C) conversion efficiency. In this mechanism, the amplitude of the THz emission is highly dependent on the S2C conversion efficiency. Recently, it has been shown that THz emitters can be designed using a single

FM layer, which utilizes the anomalous Hall effect (AHE) phenomenon [20–23]. On the one hand, the UDM mechanism relies on bulk properties of a single FM layer, while on the other hand the AHE mechanism corresponds to a combined effect of interface and bulk properties, which will be further discussed below.

A fs laser pulse when incident on a FM layer will excite hot electrons in the FM layer. The system achieves equilibrium through electron-electron, electron-phonon and electron-magnon interactions. Before attaining the equilibrium with respect to electron-electron interactions, the hot electrons acquire a velocity of order  $10^6$  m/s and move within the FM layer in a super-diffusive manner [24, 25]. When reaching the FM/dielectric interfaces as indicated in Fig. 1, electrons reflect back from the interfaces to form a net backflow current ( $j_{bf}$ ) along the film thickness direction [25]. In the presence of the AHE,  $j_{bf}$  is converted to a transient current ( $j_t$ ) defined as  $j_t = \theta_{AHE}(m \times j_{bf})$ , where  $\theta_{AHE}$  and  $m$  are the anomalous Hall angle and the magnetization direction, respectively. The net backflow current depends on the dielectric properties of the interfaces, their roughness and properties of the FM layer, such as  $\theta_{AHE}$  and  $m$ .

Recently, Zhang *et al.* [21] reported the THz emission in FM layers with different  $\theta_{AHE}$ , where  $(\text{Fe}_{0.8}\text{Mn}_{0.2})_{0.67}\text{Pt}_{0.33}$  (FeMnPt) with  $\theta_{AHE}=0.0269$  was found to exhibit the largest THz emission. However, in the same study, the THz amplitude was found to be much smaller for  $\text{Co}_{0.2}\text{Fe}_{0.6}\text{B}_{0.2}$  even though the anomalous Hall angle for  $\text{Co}_{0.4}\text{Fe}_{0.4}\text{B}_{0.2}$  is of the same order of magnitude ( $\theta_{AHE}^{\text{CoFeB}} \sim -0.023$ ) as that of FeMnPt [23]. Moreover, NiFe was found to exhibit larger THz emission than  $\text{Co}_{0.2}\text{Fe}_{0.6}\text{B}_{0.2}$ , which is in contradiction with results reported by Seifert *et al.* [14]. Note that the latter study utilized the iSHE mechanism for THz generation. Liu *et al.* [22] managed to distinguish and separate the different contributions to the THz radiation, where they demonstrated that the UDM mechanism (magnetic dipole) is linearly dependent on the FM layer thickness while the AHE mechanism is not. In addition, the composition of the FM layer defines the magnitude of  $\theta_{AHE}$ ,

\* peter.svedlindh@angstrom.uu.se

† rahul.gupta@angstrom.uu.se

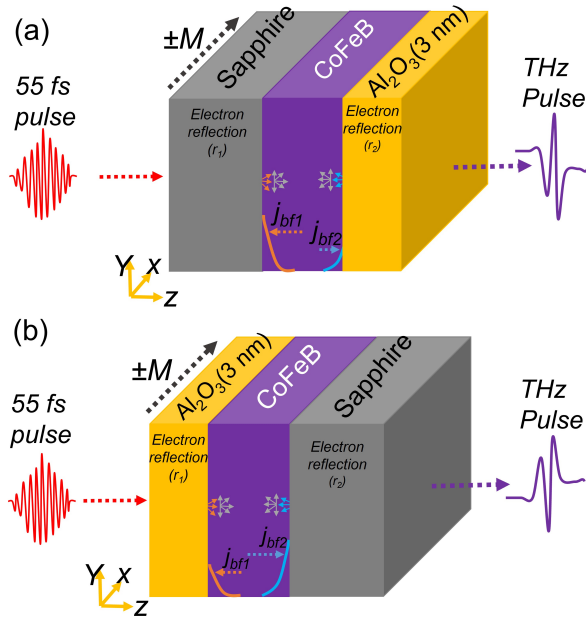


FIG. 1. Schematic of THz emission from the AHE-based CoFeB emitter. (a) pumping from the substrate side and (b) pumping from capping side.

which is a major factor in AHE-based THz emitters [20]. However, a systematic study providing direct evidence of the relationship between the anomalous Hall angle and the terahertz emission in single FM layers is still missing.

In this study, we used  $\text{Co}_{0.4}\text{Fe}_{0.4}\text{B}_{0.2}$  (CoFeB) as the AHE layer to reveal the impact of the AHE on the THz emission. We provide direct evidence for the relationship between the AHE and the THz emission in CoFeB, by presenting results from systematic studies of the effect of the CoFeB thickness on the anomalous Hall resistivity, anomalous Hall angle and the anomalous Hall coefficient. In addition, we also reveal the mechanism behind the AHE in CoFeB.

## II. EXPERIMENTAL DETAILS

Thin films of CoFeB with different thicknesses ( $t_{\text{CoFeB}}$ ) were deposited at room temperature using a DC magnetron sputtering system equipped with a turbo pump achieving a base pressure of  $1 \times 10^{-10}$  Torr. The base pressure and working pressure of the chamber during deposition were  $5 \times 10^{-10}$  and  $2 \times 10^{-3}$  Torr, respectively where 99.999% pure Ar gas was used as a sputtering gas. Prior to the deposition, the single-side polished  $\text{Al}_2\text{O}_3$  substrates (thickness  $\sim 0.5$  mm) were preheated at base pressure to  $600^\circ\text{C}$  for one hour and then cooled down to room temperature before deposition. Substrates were rotated at 6 rpm speed for uniform growth. The deposition rate of CoFeB was calibrated using X-ray re-

flectivity (XRR) measurements. To protect the CoFeB layer from oxidation and provide an additional interface for the backflow current, a 3 nm thick Al cap layer was deposited.

The deposited CoFeB films were investigated by X-ray diffraction as well as XRR with  $\text{Cu K}\alpha$  radiation. It was found that all CoFeB films are amorphous in nature and that the interface roughness is larger for the cap/CoFeB interface than for the CoFeB/substrate interface, which provides a net backflow current. Details are described in section 1 of supplementary materials (SM) [26].

A THz time-domain spectrometer was used to measure the THz emission from the CoFeB films [15, 27, 28]. A Spectra-Physics Tsunami (Ti: sapphire) was used as a laser source, which delivers pulses of  $\sim 55$  fs duration (bandwidth  $\sim 12$  nm, central wavelength  $\sim 800$  nm, and maximum output energy  $\sim 10$  nJ) at a repetition rate of 80 MHz. A low-temperature gallium arsenide photoconductive dipole antenna with  $\sim 4\mu\text{m}$  gap was used as a detector for the THz pulses. A probe beam with average laser power of 10 mW was used for detection and a static in-plane magnetic field of  $\sim 85$  mT was used to saturate the magnetization of the CoFeB films. The displayed THz signals in the figures correspond to averages of 500 detected THz spectra obtained within one minute of measurement time (cf. Fig. S2 in SM [26]).

The Quantum Design physical property measurement and magnetic properties measurement systems were employed to measure the AHE and the saturation magnetization of the CoFeB-based emitters, respectively. For AHE measurements, Hall bar devices ( $20 \times 100 \mu\text{m}^2$ ) were patterned using optical lithography.

## III. RESULTS AND DISCUSSION

Figure 1 illustrates a schematic of THz emission from AHE-based CoFeB emitters when the laser pulse is irradiated from the substrate and capping sides. Due to different interface roughness (cf. section 1, SM [26]), a net backflow current is expected. According to the relation  $j_t = \theta_{\text{AHE}} (m \times j_{\text{bf}})$ , the direction of the net backflow current depends on two factors; the direction of magnetization ( $m$ ) and the direction of the pumping side (i.e., laser pumping either from the substrate side or the capping side).

Terahertz emission due to the iSHE can be neglected, since there is no heavy metal with large spin-orbit coupling (i.e., high S2C conversion efficiency) in our films. Instead, the origin of the recorded THz emission can result from a combination of the UDM and AHE mechanisms. Figure 2(a) shows the generated THz waveforms from a substrate/CoFeB(5nm)/cap emitter with different magnetization polarities and different pumping sides. Note that the polarity of the THz waveform is reversed when reversing the magnetization direction while keeping the pumping side the same (i.e., the net backflow current direction is the same). Thus, the THz emission is

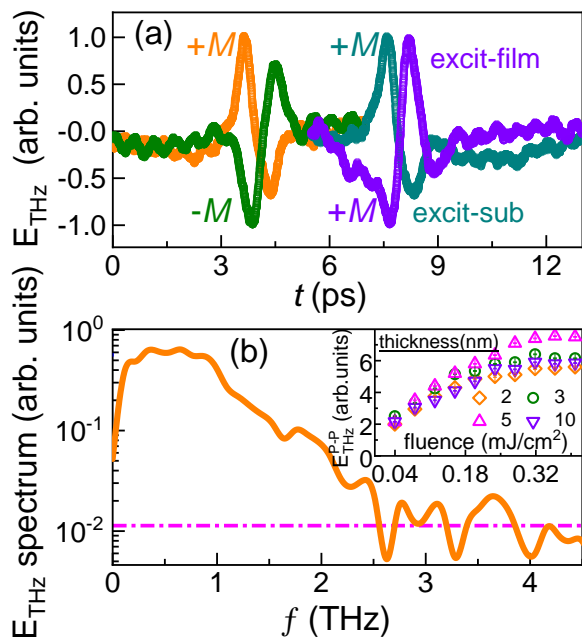


FIG. 2. (a) Left: THz waveform in time-domain ( $t$ ) for substrate/CoFeB(5 nm)/cap emitter with different magnetization directions ( $\pm M$ ) when pumping from substrate side. Right: THz waveform pumping from the capping layer and substrate sides while keeping the same magnetization direction. (b) Fast Fourier transform of THz electric field and the inset shows THz peak-to-peak amplitude for substrate/CoFeB( $t_{\text{CoFeB}}$  nm)/cap emitters as a function of pump fluence.

clearly of magnetic origin. Moreover, the THz waveform polarity is reversed when the sample is flipped, which is attributed to the AHE due to a change in direction of the net backflow current. It should be noted that the waveform polarities will be the same for the UDM mechanism due to similar magnetization dynamics. Thus, this clearly indicates that the dominant THz emission mechanism for the CoFeB emitters is the AHE, which is a combination of bulk and interface effects. The dependence of the THz peak-to-peak amplitude ( $E_{THz}^{P-P}$ ) on the laser pump fluence is shown in the inset of Fig. 2(b). Note that  $E_{THz}^{P-P}$  shows a linear behaviour up to  $0.18 \text{ mJ}/\text{cm}^2$  pump fluence, thus the pump fluence was fixed at  $0.18 \text{ mJ}/\text{cm}^2$  for the thickness-dependent study as discussed below.

The CoFeB thickness dependence of the AHE was measured to further investigate the relationship between the THz emission and the AHE. A schematic of the AHE measurement using a Hall bar geometry is depicted in the inset of Fig. 3(b). A longitudinal DC current (4 mA) was applied and the transverse voltage (i.e., Hall voltage) was measured while sweeping the out-of-plane magnetic field. The Hall resistivity ( $\rho_{xy}$ ) contains contributions from the AHE and the ordinary Hall effect. The anomalous Hall resistivity ( $\rho_{xy}^{AH}$ ), defined as the sat-

uration value of  $\rho_{xy}$ , was extracted after subtracting the contribution from the ordinary Hall effect; the thickness dependence of  $\rho_{xy}^{AH}$  is shown in Fig. 3(b). The CoFeB thickness dependence of the longitudinal resistivity ( $\rho_{xx}$ ) was also measured, which follows an exponential behavior as shown in Fig. 3(c). The ratio of the anomalous Hall resistivity to the longitudinal resistivity defines the anomalous Hall angle ( $\theta_{AHE} = \rho_{xy}^{AH}/\rho_{xx}$ ). A comparison of the  $\theta_{AHE}$  and the THz peak-to-peak amplitude as a function of CoFeB thickness is shown in Fig. 3(d). Both  $\theta_{AHE}$  and  $E_{THz}$  increase and follow a similar trend up to about 5 nm CoFeB thickness. However, while  $\theta_{AHE}$  saturates with a further increase of CoFeB thickness,  $E_{THz}^{P-P}$  decreases. The increase of the THz emission amplitude up to 5 nm CoFeB thickness may also be explained by that the applied field ( $\sim 85 \text{ mT}$ ) during the THz emission experiment is not sufficient to completely saturate the CoFeB films as CoFeB may possess an out-of-plane or easy cone anisotropy in the low thickness regime. Therefore, in-plane magnetization hysteresis loops were measured for all films, clearly showing that this is not a valid explanation for the studied films; the magnetization for all CoFeB films saturates at magnetic fields smaller than  $85 \text{ mT}$  (cf. Fig. S4 in SM [26]). The decrease of the THz emission amplitude at larger CoFeB thickness can be explained by the fact that the spin current generated by the laser pulse scales as  $A/t_{\text{CoFeB}}$  [15], where  $A$  is the absorbance of the incident pump pulse by the emitter and  $t_{\text{CoFeB}}$  is the thickness of the CoFeB layer. Therefore, the absorbance of the incident laser pulse was calculated by measuring the incident ( $P_{inc}$ ), reflected ( $P_{ref}$ )

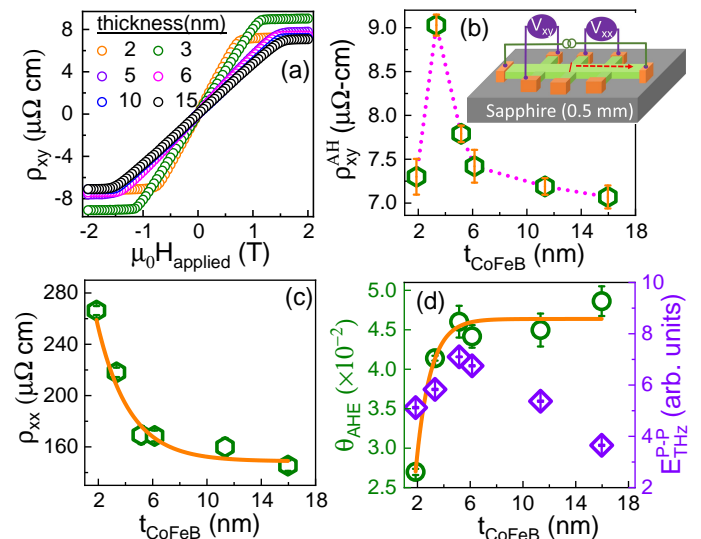


FIG. 3. Results from Hall ( $\rho_{xy}$ ) and longitudinal ( $\rho_{xx}$ ) resistivity measurements on CoFeB films with different thickness. (a)  $\rho_{xy}$  vs. applied magnetic field ( $\mu_0 H_{\text{applied}}$ ), (b)  $\rho_{xy}^{AH}$  vs.  $t_{\text{CoFeB}}$  where  $\rho_{xy}^{AH}$  corresponds to the saturation value of  $\rho_{xy}$ , (c)  $\rho_{xx}$  vs.  $t_{\text{CoFeB}}$ , and (d) THz peak-to-peak amplitude (right y-axis) and anomalous Hall angle (left y-axis) vs.  $t_{\text{CoFeB}}$ .

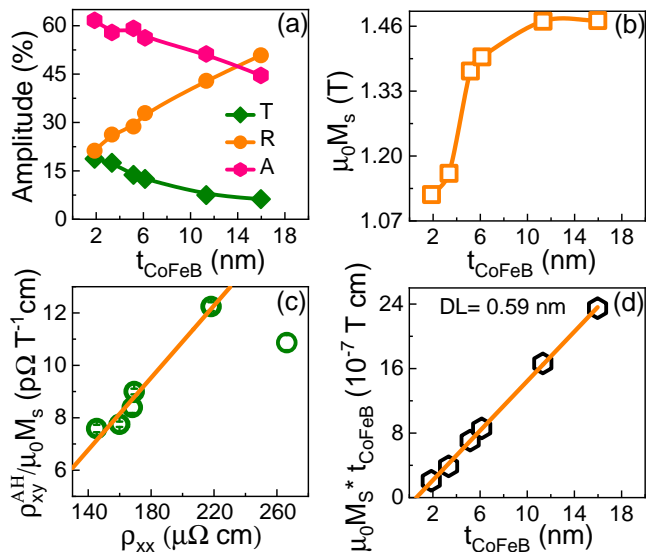


FIG. 4. (a) Transmission ( $T$ ), reflectance ( $R$ ) and absorbance ( $A$ ) vs.  $t_{\text{CoFeB}}$ . Solid lines are shown as guide to the eye. (b) Saturation magnetization  $\mu_0 M_s$  vs.  $t_{\text{CoFeB}}$ . Solid line is shown as guide to the eye. (c)  $\rho_{xy}^{\text{AH}}/\mu_0 M_s$  vs.  $\rho_{xx}$ . Solid line is a linear fit excluding the result for the 2 nm thick film. (d)  $\mu_0 M_s \cdot t_{\text{CoFeB}}$  vs.  $t_{\text{CoFeB}}$ . Solid line is a linear fit to the experimental data.

and transmitted ( $P_{\text{trans}}$ ) powers in the optical range for all CoFeB films. The absorbance was calculated from  $A = 1 - T - R$ , where  $T = P_{\text{trans}}/P_{\text{inc}}$  and  $R = P_{\text{ref}}/P_{\text{inc}}$  are the transmittance and reflectance, respectively. The absorbance as a function of CoFeB thickness is shown in Fig. 4(a), which decreases from 60% to 45% as the CoFeB thickness increases. Note that the change in absorbance ( $\sim 33\%$ ) is not enough to explain the decrease of the THz emission ( $\sim 2$  times). Instead the results show that the decrease of the THz emission amplitude is dominated by the thickness effect (i.e., the Fabry-Perot cavity effect [14, 15]).

The experimental results confirm that the dominant mechanism for THz emission in CoFeB is the AHE. However, the AHE can have both intrinsic and extrinsic contributions. The intrinsic contribution for the AHE arises from the electronic band structure and the Berry phase [29], which generally requires growth of epitaxial layers. A dominant intrinsic contribution to the AHE in our case is unlikely since the CoFeB films are amorphous in nature (cf. section 1, SM [26]). Moreover, the extrinsic contribution originates from impurity scatterings such as side jump and skew scattering [29]. The anomalous Hall resistivity is expected to be proportional to the satura-

tion magnetization ( $M_s$ ) [29], i.e.,  $\rho_{xy}^{\text{AH}} = R_s M_s$ , where  $R_s$  is the anomalous Hall coefficient.  $R_s$  increases linearly with  $\rho_{xx}$  for skew scattering (i.e.,  $R_s \propto \rho_{xx}$ ), while the dependence is parabolic for side jump scattering (i.e.,  $R_s \propto \rho_{xx}^2$ ). Therefore, the CoFeB thickness dependence of  $M_s$  was measured to be able to identify the dominant scattering mechanism for CoFeB; the results are shown in Fig. 4(b). Figure 4(c) shows  $\rho_{xy}^{\text{AH}}/M_s$  versus  $\rho_{xx}$ , indicating a linear relationship. The deviation for the 2 nm thick CoFeB emitter is explained by the electrical transport in such low thickness is dominated by surface scattering and that the surface scattering contribution to the AHE may not be an efficient mechanism for AHE since it is mostly spin-independent [20]. The argument of the small thickness for this film is reinforced by considering the effect of the magnetically dead layer (DL = 0.59 nm) indicated by Fig. 4(d).

#### IV. CONCLUSION

To summarize, we provide direct evidence of THz emission in CoFeB thin films, which is a consequence of the anomalous Hall effect. The THz emission from single layer CoFeB films has been studied as a function of CoFeB thickness and the laser pump fluence. It is shown that the THz emission is a result of the nonthermal spin-polarized currents created by the laser pulse, which are reflected at the interfaces of the ferromagnetic layer, forming a net backflow current that is converted to a transverse charge current via the anomalous Hall effect. Results from electrical transport measurements show that the anomalous Hall angle increases with an increase of CoFeB layer thickness up to about 5 nm of CoFeB, after which it saturates with further increase of the thickness. This can be contrasted with the thickness dependence of the emitted THz amplitude, for which the increase up to about 5 nm is superseded by a decrease due to the Fabry-Perot cavity effect. Lastly, a detailed analysis of the results obtained from electrical transport measurements indicates that skew scattering is the dominant mechanism in our anomalous Hall effect-based CoFeB THz emitter.

#### V. ACKNOWLEDGMENTS

This work is supported by the Swedish Research Council (grant numbers 2021-04658, 2018-04918, and 2017-03725) and Olle Engkvists Stiftelse (grant number 182-0365).

- [1] G. Valušis, A. LISAUSKAS, H. Yuan, W. Knap, and H. G. Roskos, *Sens.* **21**, 4092 (2021).  
 [2] J. Federici and L. Moeller, *J. Appl. Phys.* **107**, 6 (2010).

- [3] P. R. Smith, D. H. Auston, and M. C. Nuss, *IEEE Journal of Quantum Electronics* **24**, 255 (1988).

- [4] M. Venkatesh, K. Rao, T. Abhilash, S. Tewari, and A. Chaudhary, *Optical Materials* **36**, 596 (2014).
- [5] S. Lepeshov, A. Gorodetsky, A. Krasnok, E. Rafailov, and P. Belov, *Laser & Photonics Reviews* **11**, 1600199 (2017).
- [6] M. Jazbinsek, U. Puc, A. Abina, and A. Zidansek, *Applied Sciences* **9**, 882 (2019).
- [7] S. Vedyappan, A. K. Chaudhary, V. Mottamchetty, R. Arumugam, V. Gandhiraj, M. Senthil Pandian, and R. Perumalsamy, *Crystal Growth & Design* **19**, 6873 (2019).
- [8] Z. Yang, L. Mutter, M. Stillhart, B. Ruiz, S. Aravazhi, M. Jazbinsek, A. Schneider, V. Gramlich, and P. Guenter, *Advanced Functional Materials* **17**, 2018 (2007).
- [9] K.-Y. Kim, J. H. Glowonia, A. J. Taylor, and G. Rodriguez, *Optics express* **15**, 4577 (2007).
- [10] D. Yan, Y. Wang, D. Xu, P. Liu, C. Yan, J. Shi, H. Liu, Y. He, L. Tang, J. Feng, *et al.*, *Photonics Research* **5**, 82 (2017).
- [11] C. Lu, C. Zhang, L. Zhang, X. Wang, and S. Zhang, *Phys. Rev. A* **96**, 053402 (2017).
- [12] J. D. Bagley, C. D. Moss, S. A. Sorenson, and J. A. Johnson, *Journal of Physics B: Atomic, Molecular and Optical Physics* **51**, 144004 (2018).
- [13] J. A. Fülöp, S. Tzortzakis, and T. Kampfrath, *Advanced Optical Materials* **8**, 1900681 (2020).
- [14] T. Seifert, S. Jaiswal, U. Martens, J. Hannegan, L. Braun, P. Maldonado, F. Freimuth, A. Kronenberg, J. Henrizi, I. Radu, *et al.*, *Nat. Photonics* **10**, 483 (2016).
- [15] R. Gupta, S. Husain, A. Kumar, R. Brucas, A. Rydberg, and P. Svedlindh, *Adv. Opt. Mater.* **9**, 2001987 (2021).
- [16] E. Beaurepaire, J.-C. Merle, A. Daunois, and J.-Y. Bigot, *Phys. Rev. Lett.* **76**, 4250 (1996).
- [17] W. Zhang, P. Maldonado, Z. Jin, T. S. Seifert, J. Arabski, G. Schmerber, E. Beaurepaire, M. Bonn, T. Kampfrath, P. M. Oppeneer, *et al.*, *Nature communications* **11**, 1 (2020).
- [18] E. Beaurepaire, G. Turner, S. Harrel, M. Beard, J.-Y. Bigot, and C. Schmuttenmaer, *Applied Physics Letters* **84**, 3465 (2004).
- [19] T. Kampfrath, M. Battiato, P. Maldonado, G. Eilers, J. Nötzold, S. Mährlein, V. Zbarsky, F. Freimuth, Y. Mokrousov, S. Blügel, *et al.*, *Nature nanotechnology* **8**, 256 (2013).
- [20] Y. Yang, Z. Luo, H. Wu, Y. Xu, R.-W. Li, S. J. Pennycook, S. Zhang, and Y. Wu, *Nature communications* **9**, 1 (2018).
- [21] Q. Zhang, Z. Luo, H. Li, Y. Yang, X. Zhang, and Y. Wu, *Phys. Rev. Applied* **12**, 054027 (2019).
- [22] Y. Liu, H. Cheng, Y. Xu, P. Vallobra, S. Eimer, X. Zhang, X. Wu, T. Nie, and W. Zhao, *Phys. Rev. B* **104**, 064419 (2021).
- [23] G. Su, Y. Li, D. Hou, X. Jin, H. Liu, and S. Wang, *Phys. Rev. B* **90**, 214410 (2014).
- [24] M. Battiato, K. Carva, and P. M. Oppeneer, *Phys. Rev. Lett.* **105**, 027203 (2010).
- [25] M. Battiato, K. Carva, and P. M. Oppeneer, *Phys. Rev. B* **86**, 024404 (2012).
- [26] Supplementary Material is available for this article.
- [27] R. Gupta, E. Bagherikorani, V. Mottamchetty, M. Pavelka, K. Jatkar, D. Dancila, K. Mohammadpour-Aghdam, A. Rydberg, R. Brucas, H. A. Dürr, *et al.*, *arXiv preprint arXiv:2110.01547* (2021).
- [28] R. Gupta, *Spin Current Generation in Magnetic Heterostructures and its Impact on Terahertz Emission: A Spin Dynamics Perspective*, *Ph.D. thesis*, Acta Universitatis Upsaliensis (2021).
- [29] N. Nagaosa, J. Sinova, S. Onoda, A. H. MacDonald, and N. P. Ong, *Rev. Mod. Phys.* **82**, 1539 (2010).